Mixed-Mode Property of Defected Ground Structure and Its Application in Balanced Network Design With Harmonic Suppression

Lin Li, JunFa Mao, *Fellow, IEEE*, Min Tang, and Haoyu Dai

***Abstract*— In this letter, the mixed-mode property of a defected ground structure (DGS) is studied based on a four-port distributed equivalent circuit model. Working mechanisms of common-mode (CM) and harmonic suppression of DGS are derived and utilized to construct this new wideband balanced power-division network with harmonic suppression. The exemplary circuit exhibits wideband equal power division performance for differential mode (DM) signals and wideband suppression for CM signals and DM harmonic.**

***Index Terms*— Common-mode (CM) suppression, defected ground structure (DGS), harmonic suppression.**

I. Introduction

NOWADAYS, balanced components have become more and more popular owing to their high common-mode (CM) suppression. In some applications, both CM noise suppression and harmonic suppression are desired, since they interfere with and deteriorate the useful signals. Recently, defected ground structures (DGSs) have been employed to suppress harmonics [1] and to filter out CM noise in balanced circuits [2]. However, in these applications, only one type of suppression is provided by DGS. Generally, DGS can not only generate CM transmission zero but also differential mode (DM) transmission zero. It is thereby theoretically possible to utilize DGSs to suppress CM noise and harmonic simultaneously. As a result, additional harmonic rejection filters can be eliminated and a more compact circuit is obtained. Unfortunately, few works have been reported to utilize both the CM and DM characteristics of DGS.

In this letter, both CM and DM suppression of DGSs are studied based on a four-port equivalent circuit composed of transmission line sections. The principles for the suppression of both CM and harmonic are derived. And a novel wideband balanced power-division network with harmonic suppression is fabricated and measured to verify the theory. The proposed configuration offers several attractive advantages, including wideband CM suppression, enhanced harmonic attenuation, and very wideband fundamental bandwidth for DM signals.

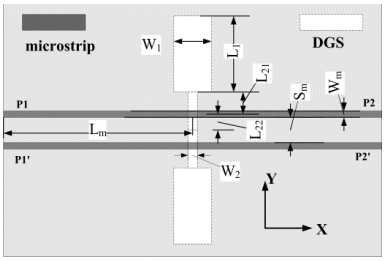

Fig. 1. Dumbbell-shaped DGS coupled balanced microstrip lines.

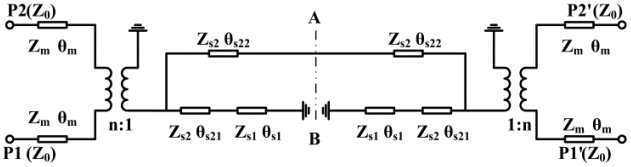

Fig. 2. Four-port equivalent circuit of DGS.

II. Theoretical Analysis

A. DM and CM Property of DGS

Fig. 1 shows the topology of a conventional dumbbell-shaped DGS on the ground plane underneath the top microstrip differential lines. Assuming a lossless whole structure, a four-port distributed circuit shown in Fig. 2 is developed to describe the mixed-mode property. The two transmission lines with characteristic impedance Z_{s1} and electrical length θ_{s1} represent the two wider slots with width W_1 and length L_1; meanwhile the two transmission lines with impedance Z_{s2} and electrical length θ_{s21} represent the two slots with width W_2 and length L_{21}; and finally the two transmission lines with impedance Z_{s2} and electrical length θ_{s22} are related to the two slots with width W_2 and length L_{22}. The electrical length of the wider and narrower slot are set to be equal, i.e., $\theta_{s1} = \theta_{s21} + \theta_{s22}$. And the impedance ratio K of the slot lines is defined as Z_{s1}/Z_{s2}. The top microstrip lines are represented by the transmission lines with impedance Z_m and electrical length θ_m. The two transformers in Fig. 2 depict

Manuscript received September 21, 2017; revised December 3, 2017; accepted January 14, 2018. Date of publication February 15, 2018; date of current version March 9, 2018. This work was supported in part by the National Natural Science Foundation of China under Grant 61361166010, Grant 51407156, Grant 61402417, and Grant 61234001 and in part by the Zhejiang Provincial Natural Science Foundation of China under Grant LY14E070009. *(Corresponding author: Lin Li.)*

L. Li is with the Key Laboratory of Ministry of Education for Design and EMC of High-Speed Electronic Systems, Shanghai Jiao Tong University, Shanghai 200240, China, and also with the College of Information, Zhejiang Sci-Tech University, Hangzhou 310018, China (e-mail: lilin_door@hotmail.com).

J. Mao and M. Tang are with the Key Laboratory of Ministry of Education for Design and EMC of High-Speed Electronic Systems, Shanghai Jiao Tong University, Shanghai 200240, China (e-mail: jfmao@sjtu.edu.cn).

H. Dai is with the College of Information, Zhejiang Sci-Tech University, Hangzhou 310018, China.

Color versions of one or more of the figures in this paper are available online at http://ieeexplore.ieee.org.

Digital Object Identifier 10.1109/LMWC.2018.2797523

1531-1309 © 2018 IEEE. Personal use is permitted, but republication/redistribution requires IEEE permission.
See http://www.ieee.org/publications_standards/publications/rights/index.html for more information.

Authorized licensed use limited to: Shanghai Jiaotong University. Downloaded on April 07,2024 at 07:50:55 UTC from IEEE Xplore. Restrictions apply.

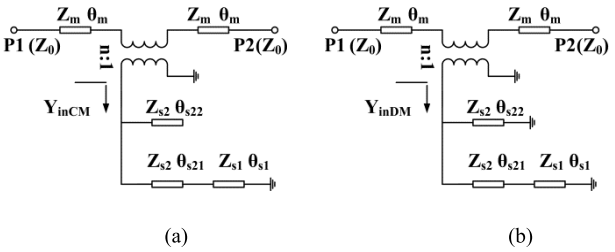

Fig. 3. (a) CM equivalent circuit of DGS. (b) DM equivalent circuit of DGS.

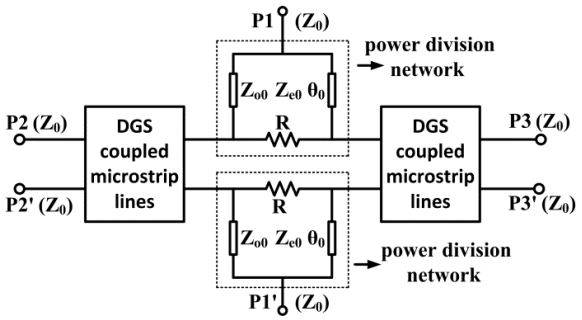

Fig. 4. Proposed balanced power-division network.

the electromagnetic coupling between the microstrip lines and the DGS. The turn ratios of the transformers can be extracted using the method presented in [3]. The equivalent half-CM and DM circuits are given in Fig. 3(a) and (b) by replacing the *AB* plane with the magnetic and electric walls, respectively.

The CM signals will be rejected at the CM rejection frequency $f_{\rm CM}$, where $Y_{\rm inCM} = 0$. $Y_{\rm inCM}$ is the CM input admittance looking into the parallel transmission lines from the transformer in Fig. 3(a). And

$$Y_{\rm inCM} = \frac{j\tan\theta_{s22}}{Z_{s2}} - \frac{j\left(Z_{s2} - Z_{s1}\tan\theta_{s21}\tan\theta_{s1}\right)}{Z_{s2}\left(Z_{s1}\tan\theta_{s1} + Z_{s2}\tan\theta_{s21}\right)}. \quad (1)$$

Relation (1) shows that at $f_{\rm CM}$ the following relation should be satisfied:

$$K = \cot^2\theta_{s1,f_{\rm CM}}. \quad (2)$$

The DM signals will be rejected at the frequency $f_{\rm DM}$ where $Y_{\rm inDM} = 0$. And

$$Y_{\rm inDM} = \frac{-j}{Z_{s2}\tan\theta_{s22}} - \frac{j\left(Z_{s2} - Z_{s1}\tan\theta_{s21}\tan\theta_{s1}\right)}{Z_{s2}\left(Z_{s1}\tan\theta_{s1} + Z_{s2}\tan\theta_{s21}\right)}. \quad (3)$$

We can get the solutions of (3) as below

$$\theta_{s1,f_{\rm DM}} = \theta_{s2,f_{\rm DM}} = \pi/2. \quad (4)$$

From the above derivation, CM noise at midband frequency f_0 and DM harmonic at nf_0 can be suppressed at the same time by letting $f_{\rm CM} = f_0$ and $f_{\rm DM} = nf_0$. In addition, the electrical length and impedance ratio can be obtained from (2) and (4).

B. Balanced Network With Harmonic Suppression

Based on the mixed-mode property of DGS, the circuit shown in Fig. 4 is utilized to construct a new balanced power-division network with both CM noise and harmonic suppression. It consists of two resistors, two DGS coupled microstrip lines, and two pairs of coupled transmission lines with $\theta_0 = \pi/2$. The CM noise and DM harmonic suppression

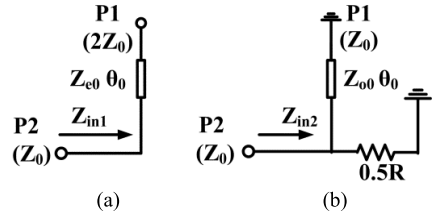

Fig. 5. (a) Even mode circuit of the power division network in Fig. 4. (b) Odd mode circuit of the power division network in Fig. 4.

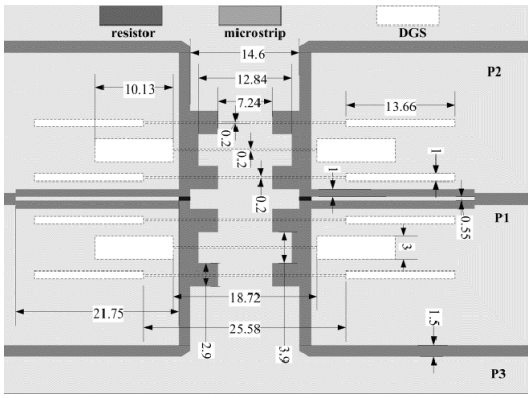

Fig. 6. Layout of the proposed balanced network (dimensions in mm).

are provided by means of the DGS coupled microstrip lines. Equal power division is realized by the power division network in Fig. 4, whose even- and odd-mode circuits are shown in Fig. 5(a) and (b), respectively. To obtain the impedance matching for all the three ports, the two input impedances of $Z_{\rm in1}$ and $Z_{\rm in2}$ in Fig. 5 should be equal to the port impedance Z_0. By letting $Z_{\rm in1} = Z_{\rm in2} = Z_0$, we can get the solutions as

$$Z_{e0} = \sqrt{2}Z_0,\ R = 2Z_0. \quad (5)$$

C. Design Procedure

Based on the above analyses, the proposed balanced network operating at 2 GHz is designed on the 0.8-mm thick substrate with the relative dielectric constant of 4.4 and loss tangent of 0.02. To suppress both the second and third harmonics, two different kinds of DGSs with different $f_{\rm DM}$ and the same $f_{\rm CM}$ are adopted in the proposed design. The electrical parameters of DGSs at 2 GHz are calculated to be $Z_{S2,\rm DGSI} = 127.8\Omega$, $\theta_{s1,\rm DGSI} = 40°$, $\theta_{s2,\rm DGSI} = 40°$, $\theta_{s22,\rm DGSI} = 28°$, $K_{\rm DGSI} = 1.42$, $\theta_{m,\rm DGSI} = 6.75°$, $Z_{m,\rm DGSI} = 21\ \Omega$, $K_{\rm DGSII} = 3$, $\theta_{s2,\rm DGSII} = 30°$, $\theta_{s1,\rm DGSII} = 30°$, $\theta_{s22,\rm DGSII} = 28°$, $Z_{S1,\rm DGSII} = 270\ \Omega$, $\theta_{m,\rm DGSII} = 13.2°$, and $Z_{m,\rm DGSII} = 37\ \Omega$. In addition, the electrical parameters of the middle part in Fig. 4 are set to be $Z_{o0} = 70.7\ \Omega$, $Z_{e0} = 50\ \Omega$, $\theta_0 = 90°$, and $R = 100\ \Omega$ at 2 GHz.

The optimal layout of the balanced network is shown in Fig. 6. In order to provide higher suppression, two DGS I are applied. The top and bottom view of the fabricated balanced network are shown in Fig. 7(a) and (b), respectively. The actual size of the core circuit is measured as 61.14 mm × 21.95 mm, i.e., approximately 0.197 λ_g^2, where λ_g is the guided wavelength at central frequency f_0.

Authorized licensed use limited to: Shanghai Jiaotong University. Downloaded on April 07,2024 at 07:50:55 UTC from IEEE Xplore. Restrictions apply.

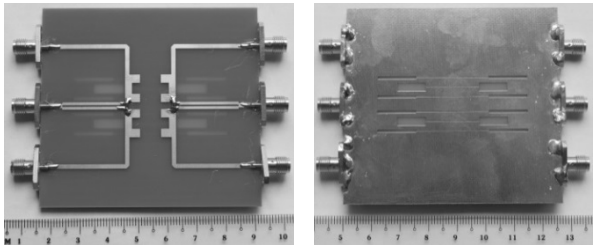

(a) (b)

Fig. 7. (a) Top view of the balanced circuit. (b) Bottom view of the balanced circuit.

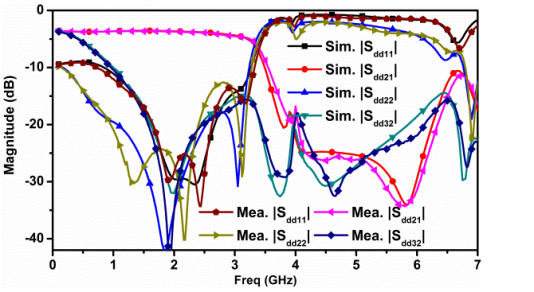

(a)

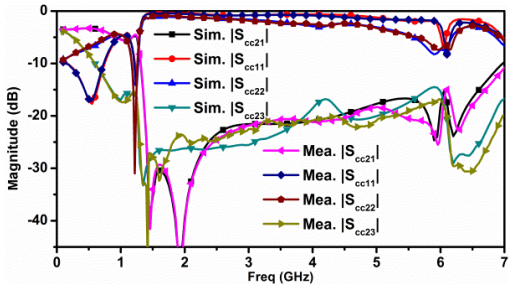

(b)

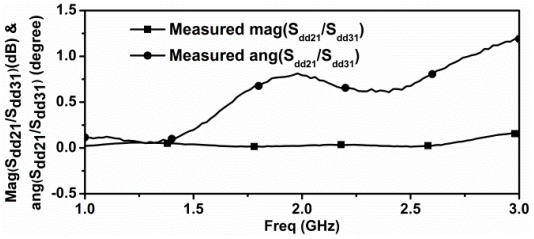

(c)

Fig. 8. (a) Simulated and measured $|S_{dd}|$. (b) Simulated and measured $|S_{cc}|$. (c) Measured magnitude and phase differences between S_{dd21} and S_{dd31}.

III. Experimental Verification

To verify the feasibility of the proposed theory, Fig. 8(a) compares the simulated and measured $|S_{dd11}|$, $|S_{dd21}|$, $|S_{dd22}|$, and $|S_{dd23}|$ while Fig. 8(b) reveals a comparison of the simulated and measured $|S_{cc11}|$, $|S_{cc21}|$, $|S_{cc22}|$, and $|S_{cc23}|$. The S-parameters are obtained by the notable commercial simulation software, ANSOFT HFSS, and are measured with the four-port vector network analyzer, Agilent E5071. Good agreement between simulation and measurement can be observed in Fig. 8. Discrepancy in Fig. 8 is mainly caused by the fabrication tolerance and parasitic effect of the surface-mounted resistors. As vividly demonstrated in Figs. 8(a) and (b), for the DM signal, the measured $|S_{dd21}|$ is greater than -4 dB from 0.01 to 2.62 GHz (fractional bandwidth (FBW) 130.5%), and the measured $|S_{dd11}|$ is less than -15 dB ranging from 1.3 to 2.78 GHz (FBW 74%). Simultaneously, the measured $|S_{dd22}|$ is observed to be less than -15 dB from 0.6 to 2.7 GHz (FBW 105%), the isolation $|S_{dd23}|$ is measured to be smaller than -20 dB from 1.56 to 2.5 GHz (FBW 47%). As for the CM signal, the observed $|S_{cc21}|$ is less than -20 dB from 1.38 to 4.6 GHz (FBW 161%), and the measured $|S_{cc23}|$ is less than -20 dB from 1.25 to 5.25 GHz (FBW 200%). Besides in Fig. 8(c), differences between S_{dd21} and S_{dd31} are graphically compared, which are 0.03 dB for magnitude difference and 0.73° for phase difference at the midband frequency.

TABLE I

Performance of Previous Works and This Letter

Ref.	size (λ_g^2)	FBW $\|S_{dd11}\|$ <-15dB	FBW $\|S_{dd23}\|$ <-20dB	FBW $\|S_{cc21}\|$ <-20dB	FBW $\|S_{cc23}\|$ <-20dB
4	0.5	17%	16%	19%	27%
5	0.38	24%	20%	36%	58%
6	0.97	46%	230%	13%	230%
7	0.14	85%	44%	40%	15%
this work	0.197	74%	47%	161%	200%

Finally, to demonstrate the superiority of the designed network, the performance of previous works and this letter is summarized in Table I. As seen in Table I, the proposed balanced network exhibits competitive performance in comparison with other referred networks in [4], [4]–[7]. Besides, the proposed one exhibits the response similar to a low-pass filter for both DM and CM signals. It is observed that $|S_{dd21}|$, $|S_{cc21}|$, $|S_{dd23}|$, and $|S_{cc23}|$ at 4 GHz are -19, -21.2, -18.8, and -20.9 dB; while $|S_{dd21}|$, $|S_{cc21}|$, $|S_{dd23}|$ and $|S_{cc23}|$ at 6 GHz are -31.5, -23.5, -21.8, and -17 dB. Hence, both the second and third harmonics are successfully suppressed under either CM or DM excitations.

IV. Conclusion

In this letter, both the CM and DM property of DGS is studied based on equivalent circuit analyses. By utilizing the CM and DM transmission zeros at the same time, a balanced power-division network is designed, implemented, and tested. The proposed network exhibits wider power division, better CM suppression, as well as enhanced harmonic suppression.

References

[1] D.-J. Woo and T.-K. Lee, "Suppression of harmonics in Wilkinson power divider using dual-band rejection by asymmetric DGS," *IEEE Trans. Microw. Theory Techn.*, vol. 53, no. 6, pp. 2139–2144, Jun. 2005.

[2] W.-T. Liu, C.-H. Tsai, T.-W. Han, and T.-L. Wu, "An embedded common-mode suppression filter for GHz differential signals using periodic defected ground plane," *IEEE Microw. Wireless Compon. Lett.*, vol. 18, no. 4, pp. 248–250, Apr. 2008.

[3] C. Caloz, H. Okabe, T. Iwai, and T. Itoh, "A simple and accurate model for microstrip structures with slotted ground plane," *IEEE Microw. Wireless Compon. Lett.*, vol. 14, no. 4, pp. 133–135, Apr. 2004.

[4] L.-S. Wu, B. Xia, W.-Y. Yin, and J. Mao, "A half-mode substrate integrated waveguide ring for two-way power division of balanced circuit," *IEEE Microw. Wireless Compon. Lett.*, vol. 22, no. 7, pp. 333–335, Jul. 2012.

[5] B. Xia, L. S. Wu, and J. Mao, "A new balanced-to-balanced power divider/combiner," *IEEE Trans. Microw. Theory Techn.*, vol. 60, no. 9, pp. 2791–2798, Sep. 2012.

[6] W. J. Feng, C. Zhao, W. Che, and Q. Xue, "Wideband balanced network with high isolation using double-sided parallel-strip line," *IEEE Trans. Microw. Theory Techn.*, vol. 63, no. 12, pp. 4013–4018, Dec. 2015.

[7] J. Shi, J. Wang, K. Xu, J.-X. Chen, and W. Liu, "A balanced-to-balanced power divider with wide bandwidth," *IEEE Microw. Wireless Compon. Lett.*, vol. 25, no. 9, pp. 573–575, Sep. 2015.

Authorized licensed use limited to: Shanghai Jiaotong University. Downloaded on April 07,2024 at 07:50:55 UTC from IEEE Xplore. Restrictions apply.